


# Comparative Analysis of 3D-Printed Drill Guides and Minimally Invasive Osteosynthesis in Feline Sacroiliac Luxation: A Cadaveric Study

Radu Mircea Scortea<sup>1</sup>  Fee Marie Fohrmann<sup>1</sup> Cosmin Muresan<sup>2</sup> Alexandru Gabriel Neagu<sup>3</sup>  
Niculae Tudor<sup>3</sup> Maximiljan W. Krauss<sup>1</sup>

<sup>1</sup>Department of Surgery, Tierklinik Düsseldorf, Düsseldorf, Germany

<sup>2</sup>Department of Surgery, Anaesthesia and Intensive Care, Faculty of Veterinary Medicine, University of Agricultural Sciences and Veterinary Medicine Cluj-Napoca, Cluj-Napoca, Romania

<sup>3</sup>Department of Diagnostic Imaging, Faculty of Veterinary Science Bucharest, University of Agricultural Sciences and Veterinary Medicine Bucharest, Bucharest, Romania

Address for correspondence Radu Scortea, CertAVP, MRCVS, Tierklinik Düsseldorf, Münsterstraße 359, 40470 Düsseldorf, Germany (e-mail: radu\_scortea@yahoo.co.uk).

Vet Comp Orthop Traumatol 2025;38:282–291.

## Abstract

**Objectives** This study was conducted to evaluate the efficacy of a 3D-printed drill guide technique (3D-DGT) in facilitating sacroiliac screw placement in feline cadavers with sacroiliac luxation (SIL), compared with minimally invasive osteosynthesis (MIO). Additionally, the accuracy and precision of implant placement in relation to preoperative planning were evaluated.

**Study Design** Bilateral SIL was created in 14 feline cadavers, followed by preoperative CT scans. For both techniques, preoperative planning was performed, and 2.4-mm screws were implanted. Postoperative CT scans were then performed to evaluate screw placement accuracy, entry point translation (EPT), and the maximum angular screw deviation (MASD) in dorsal and transverse planes.

**Results** In the lateral plane, the median (IQR) EPT (in mm) with MIO significantly differed from that with 3D-DGT on the y-axis (dorsoventral direction) from the planned entry location (Mann-Whitney U test,  $U = 42.5$ ,  $Z = -2.55$ ,  $p = 0.009$ ). However, no significant differences were noted on the x-axis (craniocaudal direction) from the planned entry location (Mann-Whitney U test,  $U = 60$ ,  $Z = -1.76$ ,  $p = 0.08$ ). Median (IQR) MASD did not differ significantly between MIO and 3D-DGT in either dorsal or transverse planes (Mann-Whitney U test,  $U = 77$ ,  $Z = -0.98$ ,  $p = 0.34$ ;  $U = 64$ ,  $Z = -1.57$ ,  $p = 0.12$ , respectively).

**Conclusion** The use of 3D-DGT lead to fewer suboptimal placements compared with MIO (7.14% versus 42.85%), though the difference was not statistically significant.

## Keywords

- trauma
- comparative research
- fracture fixation techniques
- MIO (minimally invasive approach)
- fracture repair systems

## Introduction

Sacroiliac luxation (SIL) in cats accounts for 16 to 59.2% of pelvic fractures and is the consequence of a traumatic event.<sup>1–3</sup> Surgical management is recommended for non-ambulatory animals, those with a pelvic canal narrowing

>45%, or in presence of neurological deficits, pain, instability, and additional fractures along the weight-bearing axis.<sup>4,5</sup> Surgical treatment aims to realign the anatomy and restore force transmission through the sacroiliac joint, resulting in early ambulation.<sup>6</sup> Among the available treatment options,

received

August 28, 2024

accepted after revision

April 17, 2025

article published online

April 30, 2025

© 2025. Thieme. All rights reserved.

Georg Thieme Verlag KG,

Oswald-Hesse-Straße 50,

70469 Stuttgart, Germany

DOI [https://doi.org/](https://doi.org/10.1055/a-2590-9143)

10.1055/a-2590-9143.

ISSN 0932-0814.

the use of a sacroiliac screw has proven to be the most effective method for managing unilateral SIL in cats.<sup>6–9</sup> Other stabilization methods include transsacral screw fixation,<sup>9</sup> transiliac lag screw fixation or pinning,<sup>10</sup> placement of a transarticular pin secured with a tension band or iliac bone screws,<sup>11,12</sup> and tension band transiliosacral toggle suture repair.<sup>13</sup> However, complication rates associated with screw misplacement range from 12.5<sup>7</sup> to 25%<sup>14,15</sup>; these may include ventral sacral body placement and vertebral canal or intervertebral disk occupation, resulting in residual lameness<sup>16</sup> and tibial nerve palsy.<sup>17</sup> The sacral wing notch can serve as a landmark for identifying the drilling entry point in open reduction and internal fixation (ORIF), although it is present in only 34% of the feline population.<sup>6</sup> The optimal drilling angle relative to the sacral wing surface varies between  $87 \pm 7.2$  and  $107 \pm 6.8$  degrees (mean SD:  $97 \pm 6.9$  degrees).<sup>18</sup> Accurate visualization of the sacral wing surface can also be hindered if sacral fractures are present, particularly types I, II, and III.<sup>3</sup> The C-guide can facilitate sacral drilling, but its application is limited to bilateral SIL.<sup>12</sup> Intraoperative radiology<sup>8</sup> or fluoroscopy<sup>19</sup> improves screw placement accuracy in both minimally invasive osteosynthesis (MIO) and ORIF, with current data favoring MIO over ORIF.<sup>20–22</sup>

Despite a recent study demonstrating the superiority of the 3D-printed drill guide technique (3D-DGT) over the free-hand drilling technique<sup>23</sup> in repairing SIL in dogs, no study has compared 3D-DGT with MIO for sacroiliac screw placement in cats. Therefore, our study aimed to achieve two objectives: (i) to assess whether the use of 3D-DGT could facilitate the placement of screws in the feline sacrum with SIL compared with MIO; and (ii) to evaluate the accuracy and precision of implant positioning relative to preoperative planning. We hypothesized that using the 3D-DGT for sacroiliac screw placement would yield improved accuracy and precision compared with MIO.

## Materials and Methods

Ethical approval was granted by the Bioethics Committee of the Faculty of Veterinary Medicine, Bucharest, Romania.

### Cadaveric Specimens and Preparation

A total of 14 feline cadavers with a median (IQR) body weight of 2.55 (2.15–3.78) kg were used. All cadavers were preserved at  $-20^{\circ}\text{C}$  until use and were thawed at room temperature for 72 hours before the experiment. Two cadavers exhibited pathological conditions: one with diffuse idiopathic skeletal hyperostosis affecting the sacral vertebrae, and another with a transitional vertebra showing partial lumbarization of the S1. Bilateral SIL was artificially created with an impactor and a mallet, as previously described.<sup>19</sup> SIL was consistent across the cadavers, except for one case with a bilateral type I fracture of the sacrum, as classified by Anderson and Coughlan.<sup>3</sup> Each cadaver was randomized (www.random.org) to undergo 3D-DGT or MIO on the left or right side of the sacrum.

### Pre- and Postoperative CT Evaluation

CT images of each pelvis were obtained before and after implant placement using an Access CT scanner (Philips Healthcare, Suzhou, China) with a transversal helical pattern. The scanning parameters included a slice thickness of 1 mm, an increment of 0.5 mm, a matrix of  $512 \times 512$ , a pitch of 0.9375, a tube rotation time of 0.75 seconds, a voltage of 120 kV, a current of 142 mA, and bone algorithm with an edge-enhanced filter (EB). The resulting images were saved and stored in Digital Imaging and Communications in Medicine (DICOM) format for subsequent analysis.

### Preoperative Planning

Using an open-source software (3D Slicer; <https://www.slicer.org>), stereolithography (STL) models of each sacrum were extracted and transferred to a computer graphics software (Blenderfodental; <https://www.blenderfodental.com>). An experienced surgical resident (RS), under the supervision of an experienced board-certified surgeon (MK), determined the optimal sacral drilling trajectory based on the CT scan and 3D analysis of the sacrum. Blenderfodental was linked with 3D Slicer for procedural integration. A virtual screw (2.4mm diameter) representing the implant was used to plan the drill starting point and optimal trajectory through the sacral corridor (**► Fig. 1**). The virtual implant placement was planned to avoid cortical bone contact in all planes. Each implant was transformed into a virtual cylinder with a diameter matching that of the intended drill (1.8 mm diameter), and a sleeve (drill-guide component) with a length of 27 mm was created. An additional tolerance of 0.04 mm was added to prevent the drill from getting stuck in the guide (**► Fig. 2A**). At this stage, a layer with a thickness of 4 mm was created (**► Fig. 2B**) and comprised an inverted virtual representation of the lateral aspect of the sacral wing, ensuring a precise fit to the sacrum (**► Fig. 2C**). The 3D guides, along with each sacrum's STL files, were transferred to the printer software and printed in a biocompatible and autoclavable resin (Dental Ortho Model; Phrozen) using a 3D Printer (Phrozen Mighty 4K; Phrozen) with a 4K resolution ( $3840 \times 2400$ ) and of  $52\mu\text{m}$  on XY accuracy. To minimize potential errors in implant placement due to the possible presence of a previous drilling trajectory, the 3D-DGT was performed first. The time required for preoperative planning and printing was recorded.

### Surgical Technique

The cadavers were positioned in lateral recumbency, with the allocated site uppermost. For 3D-DGT, an ORIF was performed. A dorsal approach was made over the cranial dorsal iliac spine. Incisions at the caudal point of the iliac crest extended along the ilium's dorsal surface. The sacrocaudalis and middle gluteal muscles were retracted, and the sacrum and corresponding iliac wing were exposed for better visualization of the sacroiliac joint. Thorough debridement of the sacroiliac joint and removal of residual soft tissues were performed (**► Fig. 3A**). Using the 3D guide, a screw hole was drilled across the sacrum with a 1.8-mm drill bit (Arthrex

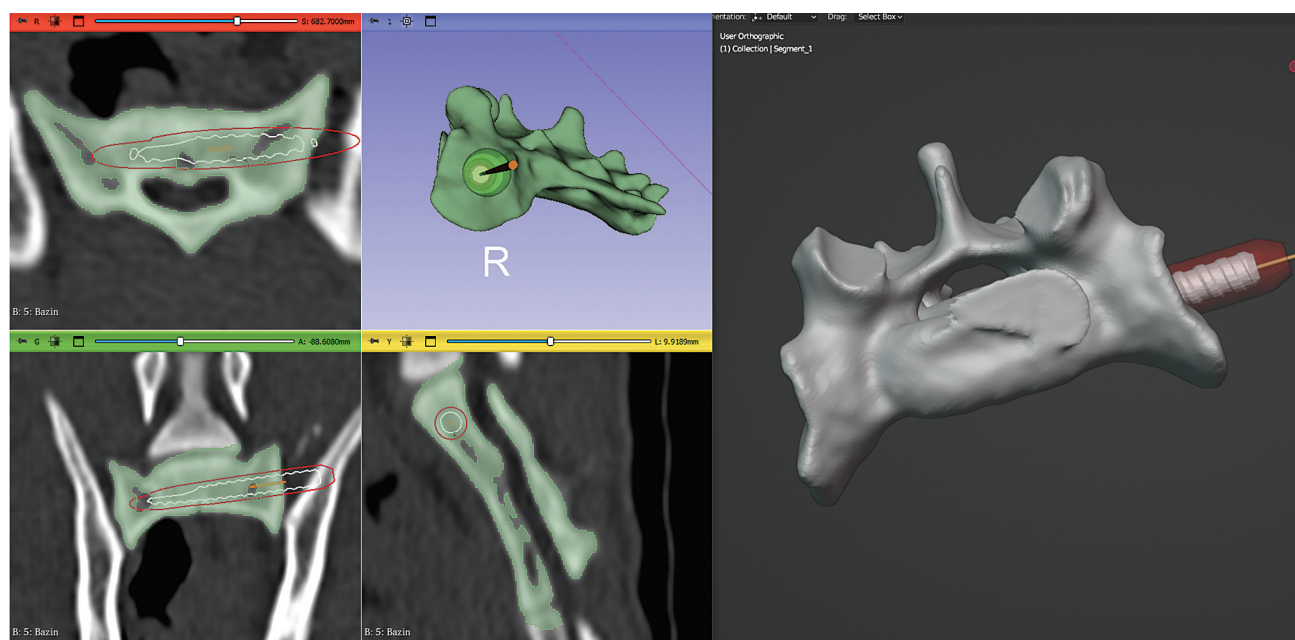


**Fig. 1** Preoperative planning, illustrating the STL models of the feline sacrum with the designed trajectories for screw placement, having the 3D Slicer (left) linked to Blenderfordental (right).

Inc., Naples, FL, USA), ensuring guide stability with manual compression (► **Fig. 3B–E**). A glide hole was drilled in the ilium from lateral to medial, and fixation was achieved using a low-profile cortical screw (2.4 mm × 20 mm Arthrex Inc., Naples, FL, USA).

MIO was performed as previously described.<sup>24,25</sup> Fluoroscopic images were obtained using a C-arm (Siemens Cios Select, Erlangen, Germany). A 0.86-mm guidewire with laser line (Arthrex Inc., Naples, FL, USA) was used as a pre-marker for drilling. Drilling was performed with a 1.7-mm cannulated drill bit (Arthrex Inc., Naples, FL, USA). Fixation was achieved using a cannulated partially threaded QuickFix Screw (2.4 × 20 mm, Arthrex Inc., Naples, FL, USA). The final screw position was confirmed fluoroscopically in lateral and dorsal planes (► **Fig. 4**). During MIO, sacral drill holes from the 3D-DGT could not be visualized under fluoroscopy. While

the 3D-DGT was performed by two experienced surgical residents (RS and FF), MIO was performed by an experienced board-certified surgeon (MK).

#### Assessment of the Postoperative CT and Comparison with Preoperative Planning

After implant placement, a pelvic CT was performed for each cadaver. Blinding of the evaluators was not feasible due to noticeable differences in the implants seen on the CT scans.

The STL files were generated for each sacrum and the corresponding implant in 3D Slicer. A segment was created defining each sacrum, with a threshold of between 370 and 390 Hounsfield Units (HU), and another segment defining the implant with a threshold of 1,350 to 1,500 HU. The files were imported into Blenderfordental and superimposed

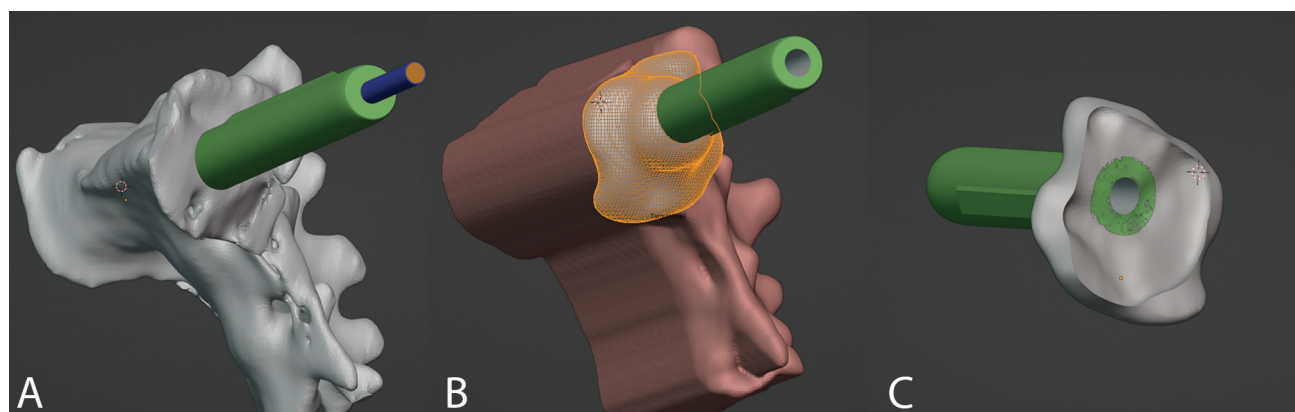


**Fig. 2** Design and fit of the 3D-DGT. The image on the left (A) shows the creation of the sleeve with a 0.04-mm tolerance gap (marked in blue). The image in the middle (B) shows the finalized design of the 3D-printed drill guide alongside its corresponding sacral model. The image on the right (C) details the inverted representation of the lateral surface of the sacrum, emphasizing the “press-fit” design.



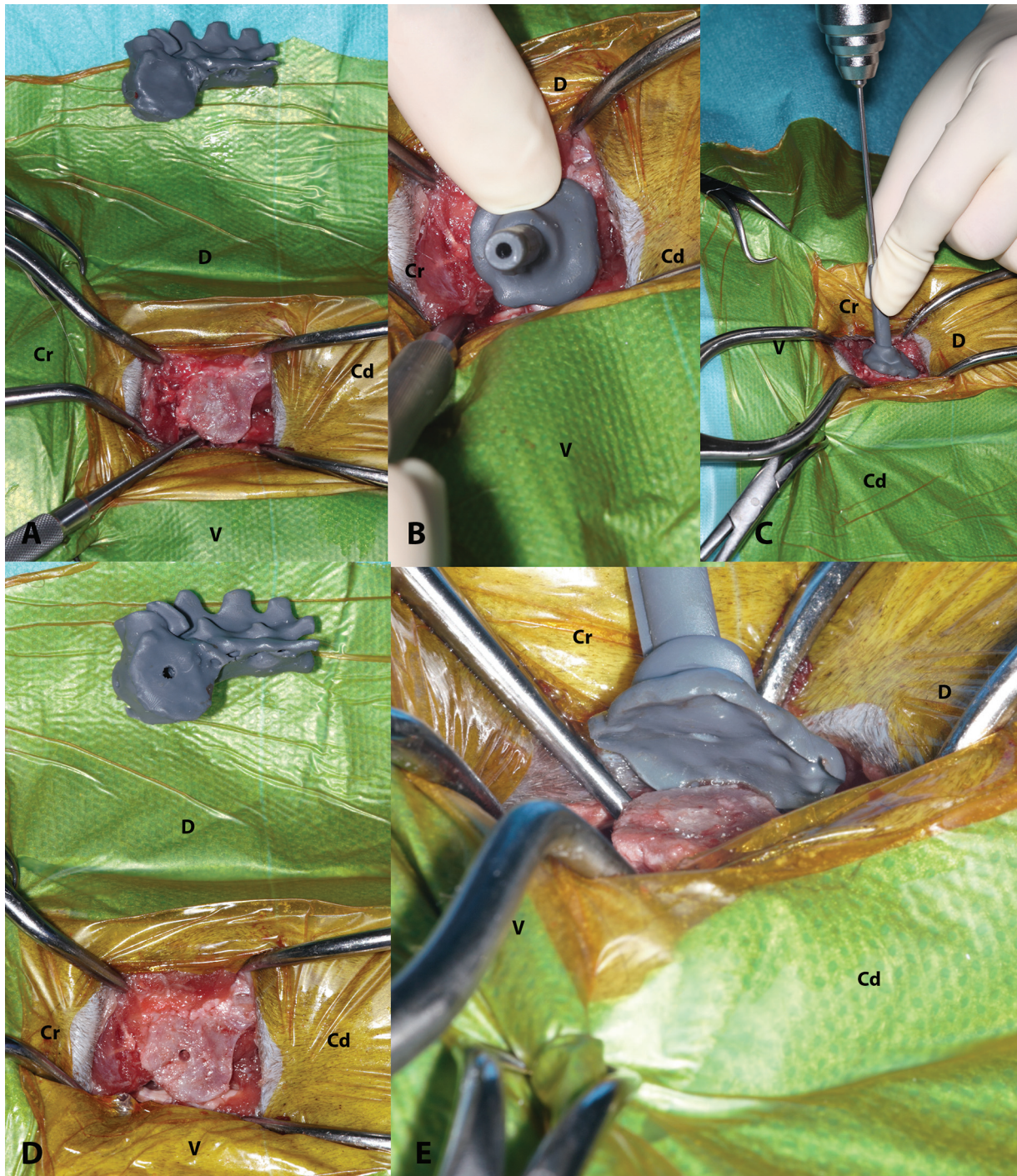


**Fig. 3** Intraoperative pictures of the 3D-DGT, illustrating the placement of the 3D guide on the sacrum and the drilling process. (A) Comparison of the 3D-printed sacrum with the prepared sacrum for drilling; (B) application of the 3D guide to the sacrum; (C) drilling of the sacrum; (D) comparison between the preplanned drilling entry point and intraoperative achieved drilling; (E) close-up image showing reasonable “press-fit” of the guide. Cd, caudal; Cr, cranial; D, dorsal; V, ventral.

using the Iterative Closest Point alignment tool. Although a quantitative registration error was not available, alignment was adjusted manually until optimal superimposition was achieved (►Fig. 5). Implant trajectories were defined by unifying the centers of a 2-mm section of each implant selected near the head of the screw and toward the tip of the shank. Pre- and postoperative angles were subsequently

measured in cross sections, and the maximum angular screw deviation (MASD) was calculated in both dorsal and transverse planes (►Fig. 6A–D). For the entry point translation (EPT) on the lateral surface of the sacrum, the center of each virtual and implanted screw was identified, and measurements were taken along the x- and y-axes to assess positional accuracy (►Figs. 6E, F and 7). The position



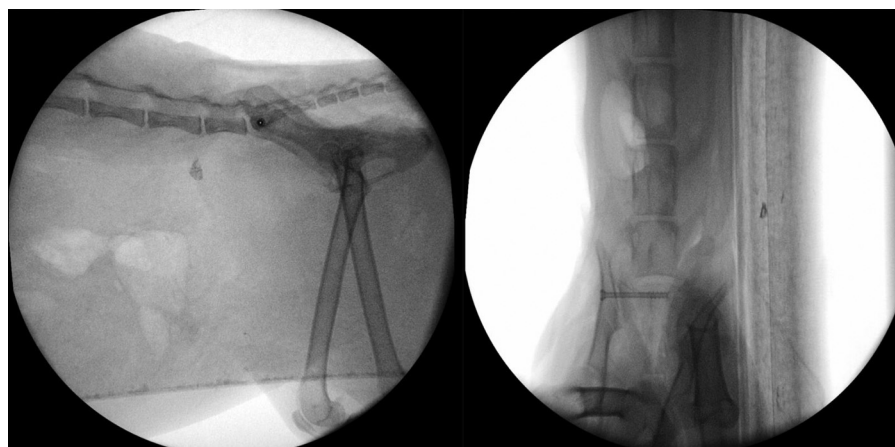


**Fig. 4** Intraoperative fluoroscopic images from MIO confirming the position of a cannulated, partially threaded 2.4 mm × 20 mm titanium QuickFix Screw (Arthrex Inc., Naples, FL, USA).

of each implanted screw was evaluated according to the criteria outlined in the modified Gras classification system<sup>26</sup> (► **Fig. 8**). Sacral bone morphometry was measured in dorsal and transverse planes. The length of each screw was assessed to determine whether it encompassed >60% purchase of the sacrum. If an implanted screw was shorter than ideal, a virtual longer implant was created and superimposed over the postoperative STL file, thus allowing the assessment of whether a longer screw would penetrate cortical bone before achieving the desired 60% sacral purchase.<sup>27,28</sup> All CT postoperative measurements were performed by one experienced surgical resident (RS) under the

supervision of an experienced board-certified surgeon (MK).

### Statistical Analysis

Statistical analyses were performed using the IBM SPSS Statistics for Windows (version 29.0.2.0 IBM Corp., Armonk, NY, USA). The data were tested for normality and found to be non-parametric. The median and interquartile range (IQR) were used to describe and summarize the data. The Mann–Whitney U test was used to compare differences between the two groups (for MASD and EPT). The Chi-square test was used to determine differences in the distribution of Gras grades between the two groups, and the Fisher exact test to assess the precision of implant placement for sacral bone purchase (SBP) and drill exit points (DEP). A *p*-value of ≤0.05 was considered statistically significant.

### Results

Following preoperative planning, 28 drilling trajectories were projected (14 trajectories per procedure). For imaging analysis, 42 CT scans were performed, accompanied by 84 measurements to assess the accuracy and precision of the drilling trajectories (lateral, dorsal, and transverse planes).

### Measurements

According to the modified Gras classification, the 3D-DGT resulted in 13/14 implants being graded as “a,” and 1/14 implant as “b II.” With the MIO, 8/14 implants were graded as “a,” 5/14 as “b” (1/14 b I and 4/14 b II), and 1/14 as “c.” The Chi-square analysis showed no statistically significant difference between the two groups (*p* = 0.09, *z* = 1.96 for 95% CI), suggesting a similar grade distribution.

For the 3D-DGT, the median (IQR) MASD was 3.05 degrees (0–5.88 degrees) in the dorsal plane and 3.4 degrees (0.29–6.6 degrees) in the transverse plane. In the dorsal plane, screw trajectories deviated caudally in 6/14 cases, cranially in 4/14, and showed no deviation in 4/14. In the transverse plane, the screw trajectory deviated ventrally in 9/14 cases, dorsally in 3/14, and showed no

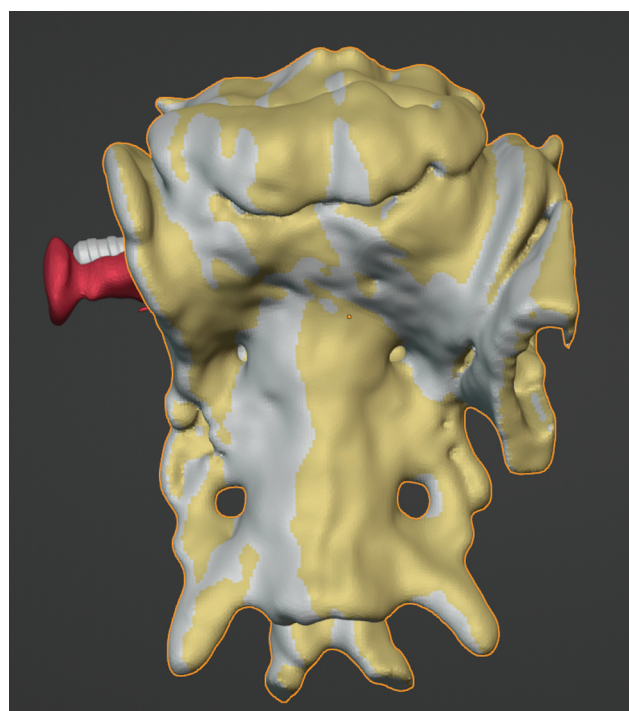


**Fig. 5** Dorsal view of the preoperative sacrum and sacroiliac implant (indicated in gray), postoperative sacrum (indicated in gold yellow), and the sacroiliac screw (indicated in red) of a cat with diffuse idiopathic skeletal hyperostosis.

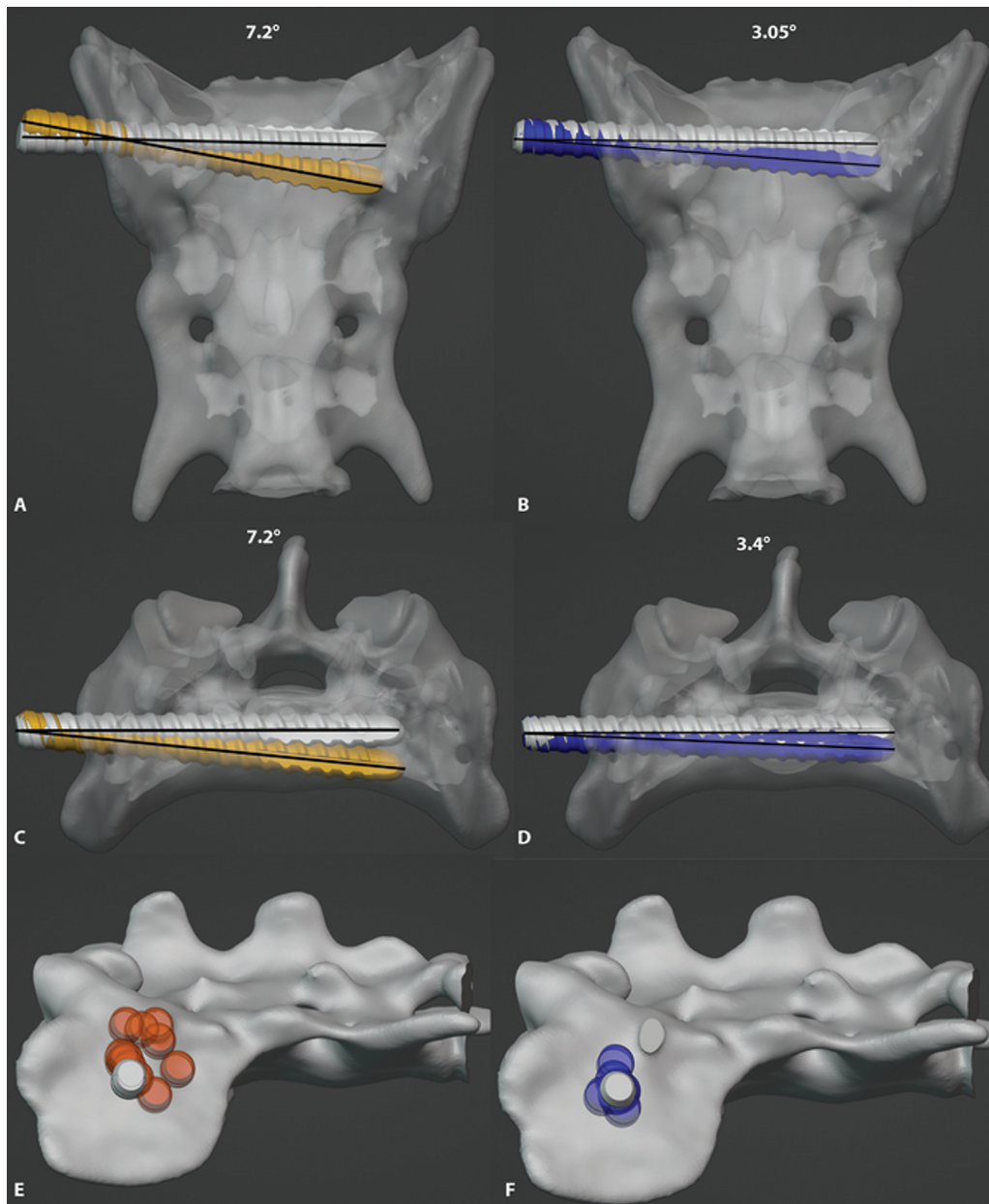


**Fig. 6** STL files of the sacrum showing median (IQR) of the angles in dorsal (A, B) and transverse planes (C, D) and the entry point translation in lateral plane (E, F) for MIO (orange screws) and 3D-DGT (blue screws). The gray screws are a representation of the preoperative planned virtual screw trajectories and insertion points.

deviation in 2/14 cases. In the lateral plane, the median (IQR) EPT from the planned entry location was 0.17 mm (0–0.36) along the x-axis (cranial–caudal direction) and 0.42 mm (0.03–0.7) along the y-axis (dorsal–ventral direction). There was no specific pattern in the screw EPT: the translation included dorsal direction (4/14), caudoventral (4/14), craniodorsal (2/14), caudodorsal (1/14), ventral (1/14), and cranial (1/14) directions. In one case (1/14) no translation occurred, and a dorsal EPT was observed in one case (1/14), graded as “b II.”

With MIO, the median (IQR) of MASD was 7.2 degrees (0–15.73 degrees) in the dorsal plane, and 7.2 degrees (2.33–13.38 degrees) in the transverse plane. In the dorsal plane,

screw trajectories deviated caudally in 8/14 cases and cranially in 4/14, with no deviation in 2/14 cases. In the transverse plane, screw trajectories deviated ventrally in 10/14 cases, dorsally in 2/14, one of which breached the vertebral canal, and showed no deviation in 2/14. In the lateral plane, the median (IQR) EPT (between virtual implant and screw) was 0.38 mm (0.07–1.87) in the cranial or caudal direction (x-axis) and 1.64 mm (0.41–3.22) in the dorsal and ventral direction (y-axis) from the planned entry location (► **Figs. 6E, F and 7**). A caudo-dorsal translation occurred in 7/14 cases, while the remaining translations were craniodorsal (3/14), dorsal (2/14), or caudoventral (2/14). All cases graded as “b” or “c” exhibited a dorsal EPT.

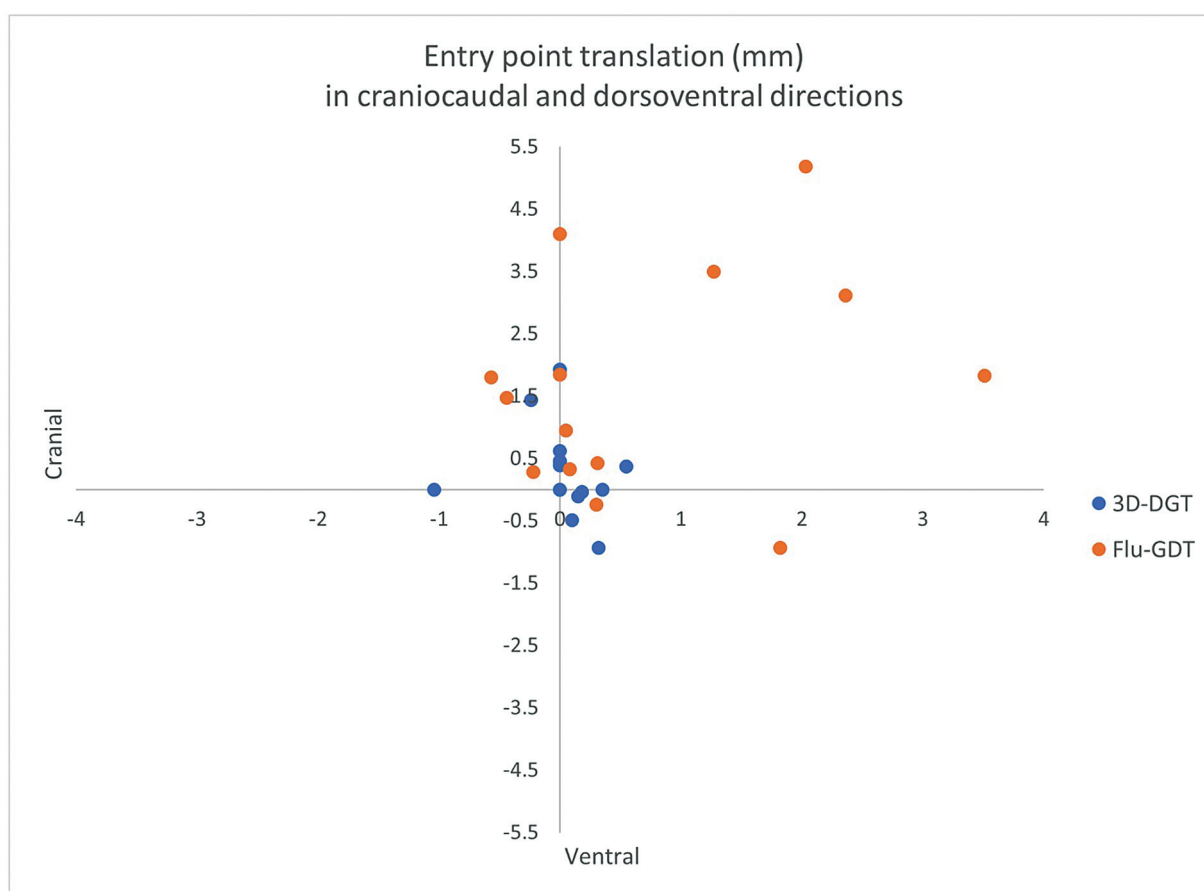


**Fig. 7** Representation of entry point translations in craniocaudal (x-axis) and dorsoventral direction (y-axis) for 3D-DGT (blue) and MIO (orange). Please note that although the figure shows 14 data points for 3D-DGT, only 13 are distinctly visible, because 4 points on the y-axis are closely clustered and overlap.

In the dorsoventral direction (y-axis), median (IQR) EPT (mm) with 3D-DGT was significantly different from that with MIO (Mann–Whitney U test,  $U = 42.5$ ,  $Z = -2.55$ ,  $p = 0.009$ ). However, no statistically significant differences were found in the median (IQR) EPT (mm) between 3D-DGT and MIO along the x-axis (craniocaudal direction) from the planned entry location (Mann–Whitney U test,  $U = 60$ ,  $Z = -1.76$ ,  $p = 0.082$ ). No statistically significant differences were detected in the median (IQR) MASD between 3D-DGT and MIO, in either the dorsal or transverse planes (Mann–Whitney U test,  $U = 77$ ,  $Z = -0.98$ ,  $p = 0.343$ ;  $U = 64$ ,  $Z = -1.57$ ,  $p = 0.120$ ). A DEP occurred in one case using 3D-DGT through the ventral cortex of the sacrum, with left-sided drilling. DEP was noted in 5/14 cadavers with MIO, with 4/14 through the ventral body of the sacrum and 1/14 dorsally in the sacral canal. Four DEPs occurred with right-sided drilling and one with left-sided drilling. With 3D-DGT, one implant exited before achieving 60% of SBP, whereas with MIO, 5/14 implants did not achieve 60% of SBP before exiting cortical bone. The Fisher exact test did not show a statistically significant difference between groups regarding the precision of SBP and DEP ( $p = 0.16$ ,  $z = 1.96$ , 95% CI). For 3D-DGT, preoperative planning required a median time (IQR) of 34 (31.75–39) minutes, while preoperative planning for MIO had a median time (IQR) of 8.5 (7–13.25) minutes.

## Discussion

Our study found that 3D-DGT achieved a smaller MASD compared with MIO in both the dorsal plane (3.05 degrees versus 7.2 degrees) and transverse plane (3.4 degrees versus 7.2 degrees). Additionally, 3D-DGT showed reduced EPT in both the x-axis (0.17 mm versus 0.38 mm) and y-axis (0.42 mm versus 1.64 mm), fewer DEP (7.14% versus 35.71%), and more consistent SBP (92.86% versus 64.29%). However, the only statistically significant difference noted was for EPT along the y-axis. Previous cadaveric and retrospective studies<sup>19,20,22</sup> have reported excellent consistency in screw placements with MIO. However, a recent clinical study<sup>14</sup> using CT revealed a 16.6% complication rate that went undetected in immediate postoperative radiographs. Another clinical study evaluating MIO in dogs and cats reported SBP >60% in only 61.5% of cases.<sup>22</sup> Most studies report safe sacroiliac implant placement using radiography in cats,<sup>8,13,24,29</sup> whereas we employed postoperative CT scanning. A recent cadaveric study on MIO found that 25% of the implants failed to achieve >60% SBP, with ventral cortical breaches noted on postoperative CT scans.<sup>15</sup> Radiography cannot assess safe implant placement in the transverse plane, leading to potential data omissions. Our study found that most errors involved ventral cortical bone breaches,



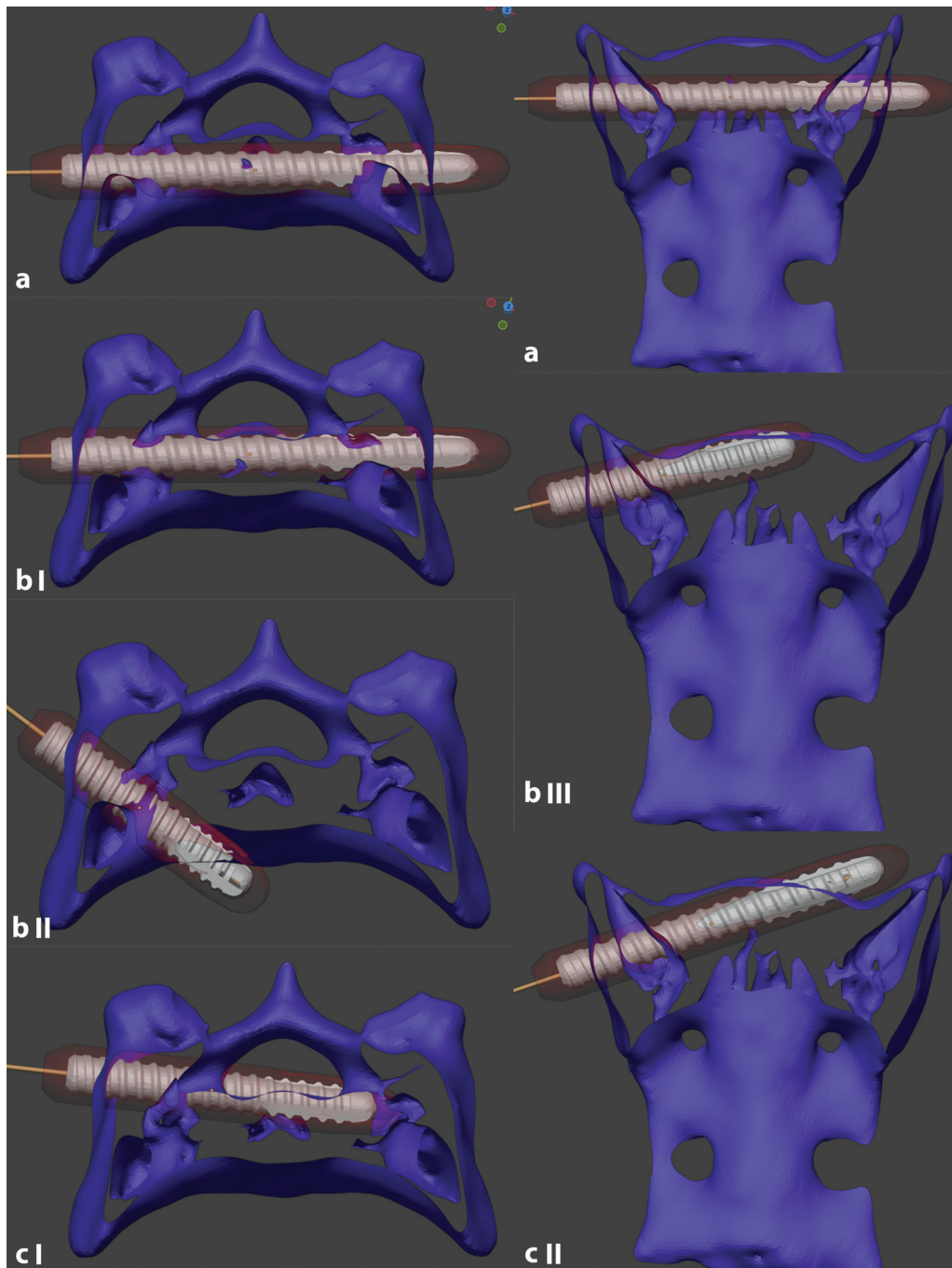


**Fig. 8** Modified Gras classification system for secure placement of implants in the sacrum. 3D representation of modified Gras scoring system in transverse plane: a, secure placement completely in cancellous bone; b I, secure placement but contacting cortical bone structures; b II, secure placement but contacting cortical structures ventrally before achieving 60% bone purchase; c I, malplacement, penetrating the cortical bone dorsally with occupation of the vertebral canal. Representation of modified Gras classification system in dorsal plane: a, secure placement, completely in cancellous bone; b III, secure placement but contacting cortical bone structures cranially before achieving 60% of bone purchase; c II, malplacement, penetrating the cortical bone cranially with occupation of intervertebral disk.

identified on transverse plane assessment. We did not find significant differences between the groups in Gras grade distribution, screw placement accuracy, or DEP. However, the small sample size may have limited the ability to detect subtle differences, suggesting that a larger sample could yield more consistent outcomes and a clearer comparison.

Anatomical variations, such as transitional vertebrae, diffuse idiopathic skeletal hyperostosis, and type I fractures,

complicate the surgical approach. Nonetheless, our study confirmed accurate screw placements using both techniques, underscoring the importance of preoperative imaging and planning of the feline sacrum, as previously recommended.<sup>14</sup>

We employed 3D measurements based on the strong correlation between CT and 3D measurements noted by McCarthy et al.<sup>23</sup> Although deviations were noted with 3D-DGT (mostly ventral: 64.29%), challenges remain in



optimal guide placement in the feline sacra. One screw placement in the 3D-DGT group was classified as “b II” due to premature ventral sacral exit. Several factors may explain these deviations, such as limitations of CT in accurately reproducing articular surfaces and the persistence of fibrocartilage attached to the sacrum in cases of sacroiliac joint disruption. Another contributing factor may be suboptimal dissection of the semilunar hyaline cartilage, which is exclusively present in the most ventral aspect of the lateral sacral wing.<sup>6</sup> This suboptimal dissection, combined with the ventral distracted iliac wing, may have impinged the guides, resulting in ventral deviations of the trajectories. Furthermore, due to the limited sacral wing surface only one implant was placed, a factor which may have further influenced the stability of the guide.

A drawback of the 3D-DGT technique is the need for more extensive soft tissue dissection to accommodate the guide, compared with standard ORIF.

In our study, the 3D-DGT technique showed a median (IQR) EPT of 0.42 mm (0.03–0.7) in the dorsal or ventral direction (y-axis), and 0.17 mm (0–0.36) in the cranial or caudal direction (x-axis), with angular deviations of 3.05 degrees (0–5.88) in the dorsal and 3.41 degrees (0.29–6.6) in the transverse planes. These angular values are similar to those observed by McCarthy et al<sup>23</sup> who reported an EPT (mean  $\pm$  SD) of  $2.4 \pm 1.4$  mm and trajectory deviations of  $3.9 \pm 3.2$  degrees in the dorsal plane and  $4.2 \pm 3.9$  degrees in the transverse plane. Comparing our results with a previous cadaveric canine study,<sup>20</sup> 3D-DGT exhibited lower maximum screw deviations in both the dorsal plane (3.05 degrees versus  $7.43 \pm 4.89$  degrees) and transverse plane (3.4 degrees versus  $8.5 \pm 5.3$  degrees) compared with traditional ORIF. However, it did not provide any advantage over MIO ( $1.59 \pm 1.08$  degrees and  $1.2 \pm 0.6$  degrees, respectively). Additionally, our MIO results showed higher median (IQR) MASD in the dorsal plane (7.2 degrees [0–15.73 degrees]) and in the transverse plane (7.2 degrees [2.33–13.38 degrees]) compared with previously reported MIO deviations.<sup>20</sup> Most of the trajectories in both groups deviated ventrally. Although a ventral screw DEP is preferable to a dorsal DEP, it is essential to recognize that an implant exiting the sacrum ventrally can potentially damage the lumbosacral plexus or median sacral vessels.<sup>8,18</sup> These ventral deviations may have resulted from the surgeon's intentional attempt to avoid DEP into the vertebral canal. From a patient's positioning perspective, MIO often necessitates complex adjustments to achieve optimal imaging angles, whereas 3D-DGT offers a more straightforward approach.

The 3D guides used for canine sacra in the aforementioned study<sup>23</sup> found deficits in achieving a “press-fit” to the lateral aspect of the sacral wing and included two additional sleeves to help with further stabilization. Contrastingly, our intraoperative placement of the guides achieved a reasonable “press-fit” to the lateral aspect of the sacral wing (► Fig. 3). Our 3D guide sleeve design incorporated a 0.04 mm tolerance, allowing smooth drill operation and minimizing debris formation, as previously recommended.<sup>30</sup> To further ensure accuracy, sleeves of 27-mm length were designed, reducing the likelihood of angled drilling.<sup>30</sup>

This study has several limitations. First, the small sample size may have restricted our ability to identify statistically significant differences between the two surgical techniques. Indeed, this is a common challenge in veterinary surgical research due to the limited availability of cadaveric specimens. The post-hoc power analysis revealed significant differences between the two groups for EPT in dorsoventral and caudocranial directions, as well as for MASD in the transverse plane, with large effect sizes (Cohen's  $d = 1.14$ , 0.89 and 0.86) and generally high statistical power (0.89, 0.72, and 0.7). However, the MASD in the dorsal plane showed smaller effect size (Cohen's  $d = 0.63$ ) and lower statistical power (0.48), suggesting that the study may have been underpowered to detect true effects for this variable. Second, variability in measurement may have resulted from fine manual adjustments that were needed after using the Iterative Closest Point alignment tool due to sacroiliac joint alignment differences between pre- and postoperative images. Third, although preoperative planning for MIO was performed in our study, it is not frequently followed in practice when intraoperative imaging is considered satisfactory, which might have influenced our results. Lastly, blinding of the evaluators was not possible as only one surgeon with the necessary expertise performed all postoperative measurements, potentially introducing bias.

## Conclusion

We propose 3D-DGT as an alternative to MIO for sacroiliac screw placement in feline cadavers. Our study found fewer suboptimal placements with 3D-DGT (7.14% versus 42.85% with MIO), though the difference was not statistically significant. Further clinical studies are needed.

### Ethical Approval Statement

Ethical approval was granted by the Bioethics Committee of the Faculty of Veterinary Medicine Bucharest, Approval Issue no. 23 17.05.2022.

### Authors' Contribution

All authors contributed to the conception, study design, acquisition of data, data analysis and interpretation. All authors drafted, revised, and approved the submitted manuscript and are publicly responsible for the relevant content.

### Funding

The authors disclose that Arthrex provided funding in the form of the implants used for the study (Study ID: IIRR-01601).

### Conflict of Interest

None declared.

### Acknowledgment

The authors are very grateful to Dr. Florin Leca and Dr. Stefan Geanta from Doctor's Vet Universe Veterinary Clinic for their assistance and for providing access to the C-arm.

## References

- 1 Bookbinder PF, Flanders JA. Characteristics of pelvic fracture in the cat: a 10-year retrospective study. *Vet Comp Orthop Traumatol* 1992;5(3):122–127
- 2 Bennett D. Orthopaedic disease affecting the pelvic region of the cat. *J Small Anim Pract* 1975;16(11):723–738
- 3 Anderson A, Coughlan AR. Sacral fractures in dogs and cats: a classification scheme and review of 51 cases. *J Small Anim Pract* 1997;38(09):404–409
- 4 Bird FG, de Vicente F. Conservative management of sacroiliac luxation fracture in cats: medium- to long-term functional outcome. *J Feline Med Surg* 2020;22(06):575–581
- 5 Averill SM, Johnson AL, Schaeffer DJ. Risk factors associated with development of pelvic canal stenosis secondary to sacroiliac separation: 84 cases (1985–1995). *J Am Vet Med Assoc* 1997;211(01):75–78
- 6 Burger M, Forterre F, Brunnberg L. Surgical anatomy of the feline sacroiliac joint for lag screw fixation of sacroiliac fracture-luxation. *Vet Comp Orthop Traumatol* 2004;17(3):146–151
- 7 Shales C, Moores A, Kulendra E, White C, Toscano M, Langley-Hobbs S. Stabilization of sacroiliac luxation in 40 cats using screws inserted in lag fashion. *Vet Surg* 2010;39(06):696–700
- 8 Silveira F, Quinn RJ, Adrian AM, Owen MR, Bush MA. Evaluation of the use of intra-operative radiology for open placement of lag screws for the stabilization of sacroiliac luxation in cats. *Vet Comp Orthop Traumatol* 2017;30(01):69–74
- 9 Kaderly RE. Stabilization of bilateral sacroiliac fracture-luxations in small animals with a single transsacral screw. *Vet Surg* 1991;20(02):91–96
- 10 Yap FW, Dunn AL, Farrell M, Calvo I. Trans-iliac pin/bolt/screw internal fixation for sacroiliac luxation or separation in cats: six cases. *J Feline Med Surg* 2014;16(04):354–362
- 11 Raffan PJ, Joly CL, Timm PG, Miles JE. A tension band technique for stabilisation of sacroiliac separations in cats. *J Small Anim Pract* 2002;43(06):255–260
- 12 Parslow A, Simpson DJ. Bilateral sacroiliac luxation fixation using a single transiliosacral pin: surgical technique and clinical outcomes in eight cats. *J Small Anim Pract* 2017;58(06):330–336
- 13 Froidefond B, Moinard M, Caron A. Outcomes for 15 cats with bilateral sacroiliac luxation treated with transiliosacral toggle suture repair. *Vet Surg* 2023;52(07):983–993
- 14 Wills DJ, Neville-Towle J, Podadera J, Johnson KA. Computed tomographic evaluation of the accuracy of minimally invasive sacroiliac screw fixation in cats. *Vet Comp Orthop Traumatol* 2022;35(02):119–127
- 15 Kleiner L, Wolf N, Precht C, Haenssger K, Forterre F, Düver P. Feline sacroiliac luxation: comparison of fluoroscopy-controlled free-hand vs. computer-navigated drilling in the sacrum—a cadaveric study. *Front Vet Sci* 2025;11:1510253
- 16 Burger M, Forterre F, Waibl H, Brunnberg L. Sacroiliac luxation in the cat. Part 2: cases and results. *Kleintierpraxis* 2005;50(05):287–297
- 17 Forterre F, Tomek A, Rytz U, Brunnberg L, Jaggy A, Spreng D. Iatrogenic sciatic nerve injury in eighteen dogs and nine cats (1997–2006). *Vet Surg* 2007;36(05):464–471
- 18 Shales CJ, White L, Langley-Hobbs SJ. Sacroiliac luxation in the cat: defining a safe corridor in the dorsoventral plane for screw insertion in lag fashion. *Vet Surg* 2009;38(03):343–348
- 19 Déjardin LM, Fauron AH, Guiot LP, Guillou RP. Minimally invasive lag screw fixation of sacroiliac luxation/fracture using a dedicated novel instrument system: apparatus and technique description. *Vet Surg* 2018;47(01):93–103
- 20 Déjardin LM, Marturello DM, Guiot LP, Guillou RP, DeCamp CE. Comparison of open reduction versus minimally invasive surgical approaches on screw position in canine sacroiliac lag-screw fixation. *Vet Comp Orthop Traumatol* 2016;29(04):290–297
- 21 Tomlinson J. Minimally invasive repair of sacroiliac luxation. *Vet Clin North Am Small Anim Pract* 2020;50(01):231–239
- 22 Rollins A, Balfour R, Szabo D, Chesvick CM. Evaluation of fluoroscopic-guided closed reduction versus open reduction of sacroiliac fracture-luxations stabilized with a lag screw. *Vet Comp Orthop Traumatol* 2019;32(06):467–474
- 23 McCarthy DA, Granger LA, Aulakh KS, Gines JA. Accuracy of a drilling with a custom 3D printed guide or free-hand technique in canine experimental sacroiliac luxations. *Vet Surg* 2022;51(01):182–190
- 24 Fischer A, Binder E, Reif U, Biel M, Bokemeyer J, Kramer M. Closed reduction and percutaneous fixation of sacroiliac luxations in cats using 2.4 mm cannulated screws—a cadaveric study. *Vet Comp Orthop Traumatol* 2012;25(01):22–27
- 25 Tomlinson J. Minimally invasive repair of sacroiliac luxation in small animals. *Vet Clin North Am Small Anim Pract* 2012;42(05):1069–1077, viii viii
- 26 Gras F, Marintschev I, Wilharm A, Klos K, Mückley T, Hofmann GO. 2D-fluoroscopic navigated percutaneous screw fixation of pelvic ring injuries—a case series. *BMC Musculoskelet Disord* 2010;11:153
- 27 Han CK, Kang J, Lee H, Kim N, Heo S. Evaluation of a screw insertion landmark for a minimally invasive repair technique in induced bilateral sacroiliac luxation in feline cadavers. *J Feline Med Surg* 2022;24(02):152–159
- 28 Ahn SY, Jeong SW. Evaluation of minimally invasive surgical reduction of sacroiliac luxation in toy breed dogs: a cadaver study. *J Vet Sci* 2022;23(02):e38
- 29 de Jong L, Proot JIJ, Pillin LJP, Janssens LAA. Minimally invasive placement of cannulated headless compression screws for reduction of sacroiliac luxation in 14 cats. *Vet Comp Orthop Traumatol* 2025;38(04):194–199
- 30 Van Assche N, Quirynen M. Tolerance within a surgical guide. *Clin Oral Implants Res* 2010;21(04):455–458